Journal of
Mechanics of
Materials and Structures

A NEW VARIABLE DAMPING SEMIACTIVE DEVICE FOR SEISMIC RESPONSE REDUCTION OF CIVIL STRUCTURES

Orlando Cundumi and Luis E Suárez

Volume 2, Nº 8 October 2007

mathematical sciences publishers

JOURNAL OF MECHANICS OF MATERIALS AND STRUCTURES
Vol. 2, No. 8, 2007

A NEW VARIABLE DAMPING SEMIACTIVE DEVICE FOR SEISMIC RESPONSE REDUCTION OF CIVIL STRUCTURES

ORLANDO CUNDUMI AND LUIS E SUÁREZ

A semiactive mechanism, called a VDSA (variable damping semiactive device), is proposed to reduce the seismic response of structures. It is composed of two fixed-orifice viscous fluid dampers installed in the form of a V whose top ends are attached to a floor and their lower ends to a collar that moves along a vertical rod. By varying the VDSA position one obtains an optimal instantaneous damping added to the structure. The position of the moving end is calculated with an algorithm based on a variation of the instantaneous optimal control theory which includes a generalized LQR (linear quadratic regulator) scheme. This modified algorithm, referred to as Qv, is based on the minimization of a performance index J quadratic in the state vector, the control force vector, and an absolute velocity vector. Two variants of the algorithm are used to present numerical simulations of the controlled seismic response of a single and a MDOF (multi-degree-of-freedom) structure.

1. Introduction

Civil engineering structures are typically designed to rely on their strength and ductility to withstand the large forces imposed on them by strong earthquakes. A number of modern mechanical devices have been proposed in the last two decades to reduce the structural response. They are known collectively as protective devices and they include added viscoelastic dampers, viscous fluid dampers, frictional dampers, tuned-mass dampers, and base isolation systems. The devices themselves and their design methodology are referred to as passive control systems. At the highest level of sophistication for seismic protection are the so called active control systems. Although these devices provide in theory the uppermost response reduction, they also required a large amount of energy to operate and their robustness and reliability are questionable.

In between these passive and active systems are the semiactive devices which, as the name indicates, combine the features of the former two protective systems. The force (and thus the energy) required to operate a semiactive device is much less than for an active system. To calculate the control forces that operate the passive devices, it is necessary to know the response of the structure by measuring it with sensors. A proper numerical algorithm processes this information and calculates how the properties of the (formerly) passive device should be modified.

Semiactive control systems have only recently been considered for applications to large civil structures. We believe that the application of these systems to civil engineering structures was first reported by Hrovat et al. [1983]. Several devices that can deliver changeable variable damping such as variable orifice dampers [Symans and Constantinou 1997; Kurata et al. 1999; Kurata et al. 2000] and hydraulics dampers [Kawashima et al. 1992; Patten et al. 1993; Sack et al. 1994; Patten et al. 1996] have been

Keywords: semiactive systems, control algorithms, earthquake engineering, seismic response, added damping.

proposed. Variable stiffness devices have also been proposed by Kobori et al. [1993], Nagarajaiah and Mate [1998], and Gluck et al. [2000]. Furthermore, numerous algorithms have been developed for selecting the appropriate damping coefficient [Yang et al. 1987; Soong 1990; Sadeck and Mohraz 1998; Cundumi 2005; Cundumi and Suárez 2006b]. The list of references is meant only to provide a few relevant examples; a comprehensive review of these systems is beyond the scope of this discussion.

The present paper describes the implementation of a VDSA device. In contrast to semiactive dampers described in the technical literature, the damper coefficient c is not controlled by modifying the size of an orifice in the piston, but by changing the position of the damper. The required damping coefficient is calculated by means of two instantaneous optimal control algorithms: the (*closed-loop control* and the *closed-open-loop control*). It is shown that both algorithms are effective in reducing the response. The damping coefficient $c(t)$ during the response can be adjusted between an upper limit $c_{\max}$ and a lower value $c_{\min}$.

This paper contains in detail the formulation and the results of a paper presented at the 9th Pan American Congress of Applied Mechanics, in Mérida, Mexico [Cundumi and Suárez 2006a].

2. The modified algorithm Qv

It is well known that the equations of motion of a structure modeled as a MDOF system and subjected to a base acceleration $\ddot{x}_g(t)$ at all its supports are given by

$$[M]_{n\times n}\{\ddot{x}(t)\} + [C]_{n\times n}\{\dot{x}(t)\} + [K]_{n\times n}\{x(t)\} = -[M]_{n\times n}\{E\}\ddot{x}_g(t), \tag{1}$$

where $[M]$, $[C]$ and $[K]$ are the mass, damping and stiffness matrix, respectively, the vectors $\{\ddot{x}(t)\}$, $\{\dot{x}(t)\}$ and $\{x(t)\}$ contain the relative (with respect to the foundation) acceleration, velocity and displacement of each dynamic degree of freedom of the structure, $\{E\}$ is the vector of influence coefficients, and n is the number of degrees of freedom. If all the degrees of freedom of the structural model coincide with the direction of the applied ground motion, then the vector $\{E\}$ is simply a vector with ones $\{I\}$.

If the structure is outfitted with r semiactive dampers, the previous equations of motion must be changed as follows:

$$[M]_{n\times n}\{\ddot{x}(t)\} + [C]_{n\times n}\{\dot{x}(t)\} + [K]_{n\times n}\{x(t)\} = -[M]_{n\times n}\{E\}\ddot{x}_g(t) + [D]_{n\times r}\{u(t)\}. \tag{2}$$

The matrix $[D]$ defines the locations of the controllers, r is the number of controllers and $\{u(t)\}$ is the r-dimensional control force vector. The location of the controllers (or the VDSA devices in our case) will be determined via a trial and error process by trying to maximize the effect of the devices. No attempt is made to determine the optimal position of the devices in an analytical way.

To solve the system of equations of motion, Equation (2), by transforming them into a set of uncoupled equations, it is convenient to change into a system of $2n$ first order differential equations. In Linear System Theory this method is referred to as the state-space representation. Introducing the following

response vector and matrices,

$$\{z(t)\} = \left\{\frac{\{x(t)\}}{\{\dot{x}(t)\}}\right\}, \qquad [A] = \left[\begin{array}{c|c} 0 & I \\ \hline -M^{-1}K & -M^{-1}C \end{array}\right],$$

$$[B] = \left[\frac{0}{M^{-1}D}\right], \qquad [H] = \left[\frac{0}{-E}\right].$$

Equation (2) can be written in the form:

$$\{\dot{z}(t)\}_{2n\times 1} = [A]_{2n\times 2n}\{z(t)\} + [B]_{2n\times 2r}\{u(t)\} + [H]_{2n\times 1}\ddot{x}_g(t).$$

To define the variation of the control forces in $\{u(t)\}$ one needs to select a control algorithm. In this study, two algorithms (closed-loop control and closed-open-loop control) have been developed based on the instantaneous optimal control theory. They are referred to here as the modified algorithms Qv. As usual, this type of algorithm is based on the minimization of a performance index J quadratic in the state vector $\{z(t)\}$ and in the control force $\{u(t)\}$. However, in the modified algorithm a quadratic form of the absolute velocity $\{\dot{x}_a(t)\}$ is added to J. A penalty on the state vector is imposed through a matrix $\boldsymbol{Q}$, on the control vector through a matrix $\boldsymbol{R}$ and on the absolute velocity vector through a matrix $\boldsymbol{Qv}$. $\boldsymbol{Q}$ and $\boldsymbol{Qv}$ are two symmetric positive semidefinite weighting matrices of size $2n \times 2n$ and $n \times n$, respectively, and $\boldsymbol{R}$ is an $r \times r$ positive definite weighting matrix. The performance index takes the form:

$$J = \int_0^{t_f} \Big[\{z(t)\}^T[\boldsymbol{Q}]\{z(t)\} + \{\dot{x}_a(t)\}^T[\boldsymbol{Q}_v]\{\dot{x}_a(t)\} + \{u(t)\}^T[\boldsymbol{R}]\{u(t)\}\Big]dt,$$

where t_f is the duration of excitation. Usually the excitation is not included in the definition of performance indices. However, it was found that for a semiactive device with variable damping such as the one presented in this work, including the excitation in the definition of J through the absolute velocity has a beneficial effect on the effectiveness of the device.

The absolute velocity vector is computed as

$$\{\dot{x}_a(t)\} = [A_v]_{n\times 2n}\{z(t)\} + \{S_v\}_{n\times 1}\dot{x}_g(t),$$

where $[A_v] = [0 \mid I]$, $\{S_v\} = \{1\}$, $[I]$ is an $n \times n$ identity matrix, $\{1\}$ is a vector of 1's of length n, and $\dot{x}_g(t)$ is the ground velocity.

The procedure to define the control and response vectors in the modified algorithm Qv can be found in [Cundumi 2005]. Here only the final results are reported.

For the closed-loop control case, the variables $\{u(t)\}$ and $\{z(t)\}$ can be obtained as follows:

$$\{u(t)\} = -\frac{\Delta t}{2}[R]^{-1}[B]^T\Big[[A_2]\{z(t)\} + [A_3]\dot{x}_g(t)\Big],$$

$$\{z(t)\} = \left[[I] + \frac{\Delta t^2}{4}[B][R]^{-1}[B]^T[A_2]\right]^{-1}\left[[T]\{d(t-\Delta t)\} - \frac{\Delta t^2}{4}[B][R]^{-1}[B]^T[A_3]\dot{x}_g(t) + \frac{\Delta t}{2}[H]\ddot{x}_g(t)\right],$$

where Δt is the constant time step, $[A_2] = [Q] + [A_v]^T[Q_v][A_v]$, $[A_3] = [A_v]^T[Q_v][S_v]$ and $\{d(t-\Delta t)\}$ contains the displacement x and the velocity $\dot{x}$ at time $t - \Delta t$.

For the closed-open-loop control case, $\{u(t)\}$ and $\{z(t)\}$ are calculated with the following equations:

$$\{u(t)\} = \frac{\Delta t}{4}[R]^{-1}[B]^T\big[[P]\{z(t)\} + \{p(t)\}\big], \tag{3}$$

$$\{z(t)\}=\left[[I]-\frac{\Delta t^2}{8}[B][R]^{-1}[B]^T[P]\right]^{-1}\left[[T]\{d(t-\Delta t)\}+\frac{\Delta t^2}{8}[B][R]^{-1}[B]^T\{p(t)\}+\frac{\Delta t}{2}[H]\ddot{x}_g(t)\right]. \tag{4}$$

In Equations (3) and (4), $[P]$ is the Riccati matrix and $\{p(t)\}$ represents the open-loop control.

$$[P] = -\big[[Q]+2[A_v]^T[Q_v][A_v]\big]\left[[I]+\frac{\Delta t^2}{8}[Q][B][R]^{-1}[B]^T\right]^{-1}$$

$$\{p(t)\} = -\left[\frac{\Delta t^2}{8}[Q][B][R]^{-1}[B]^T+[I]\right]^{-1}\left[[Q]\left[[T]\{d(t-\Delta t)\}+\frac{\Delta t}{2}[H]\ddot{x}_g(t)\right]\right.$$
$$\left.+2[A_v]^T[Q_v]\{S_v\}\dot{x}_g(t)\right]. \tag{5}$$

3. Equations of motion of SDOF structures controlled with the VDSA device

The system considered is shown schematically in Figure 1. It consists of a single degree of freedom structure (SDOF) with the proposed variable damping system installed. The dampers have fixed-constant damping coefficient Co_A and Co_B. The structure consists of a mass m distributed at the roof level, a massless frame that provides stiffness k to the system, and the natural (inherent) damping of the structure is represented by a damper with constant C_s. This coefficient can be defined as $2\xi m\omega_n$ where ξ is the inherent (original) damping ratio and ω_n is the natural frequency of the SDOF system. This model may be considered as an idealization of a one-story structure. In reality, each structural member (column, beam) of the structure contributes to the inertial (mass), elastic (stiffness), and energy dissipation (damping)

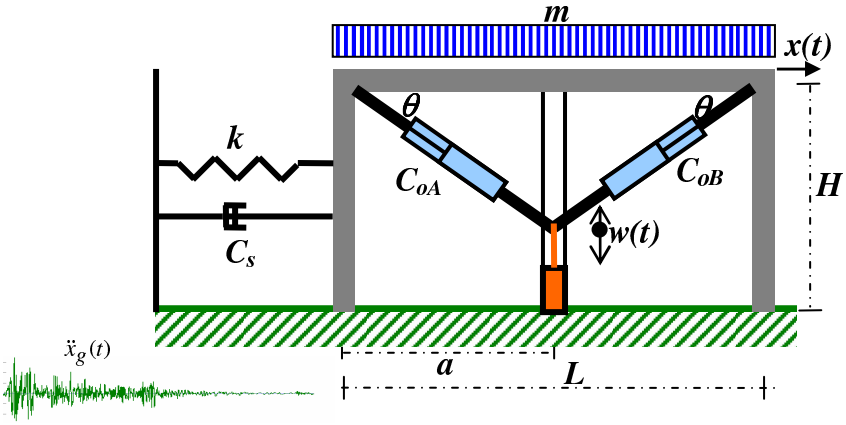

Figure 1. Single degree of freedom model of a structure with a VDSA device.

properties of the structure. In the idealized system, however, these properties are concentrated in three separate, pure components: a lumped mass, a linear spring, and a linear viscous damper.

To move the common lower end of the two dampers one needs to use an actuator, for instance a hydraulic actuator with fast reaction. The information required to determine the movement of the VDSA device includes the relative displacement and velocity of the mass m and the ground velocity $\dot{x}_g(t)$.

Figure 2 displays the velocities that govern the forces produced by the dampers: $\dot{x}(t)$ is the relative velocity of the floor and $\dot{w}(t)$ is the velocity of the bottom end of the dampers. As shown in the Figure 2, the damping force is proportional to the difference between the components of the velocities $\dot{x}(t)$ and $\dot{w}(t)$ along the axis of the dampers $\boldsymbol{A}$ and $\boldsymbol{B}$ of the VDSA device.

Using Figures 1 and 2, it can be shown that the equation of motion for the SDOF structure subjected to the horizontal component of an earthquake-induced ground acceleration is

$$m\ddot{x}(t) + \big(C_s + (C_{o_A} + C_{o_B})\cos^2\theta(t)\big)\dot{x}(t) + kx(t) = -m\ddot{x}_g(t) + \frac{1}{2}(C_{o_A} - C_{o_B})\sin 2\theta(t)\dot{w}(t), \quad (6)$$

where

$$\cos^2\theta(t) = \frac{a^2}{a^2 + [H - w(t)]^2}, \qquad \sin 2\theta(t) = \frac{2a[H - w(t)]}{a^2 + [H - w(t)]^2}, \qquad a = \frac{L}{2},$$

and a, H, and L are the dimensions shown in Figure 1.

For a structure with two dampers in a fixed position, the second term in the right hand side of the equation of motion, Equation (6), vanishes. This term arises due to the component of the velocity of the lower end of the dampers in the direction of the axis of the device. Rewriting Equation (6) in a space-state representation leads to

$$\begin{Bmatrix} \dot{z}_1(t) \\ \dot{z}_2(t) \end{Bmatrix} = \left[\begin{array}{c|c} 0 & 1 \\ \hline -m^{-1}k & -m^{-1}\big(C_s + (C_{o_A} + C_{o_B})\cos^2\theta(t)\big) \end{array}\right] \begin{Bmatrix} z_1(t) \\ z_2(t) \end{Bmatrix} + \begin{bmatrix} 0 \\ \frac{1}{2}m^{-1}(C_{o_A} - C_{o_B})\sin 2\theta(t) \end{bmatrix} \dot{w}(t) + \begin{bmatrix} 0 \\ -1 \end{bmatrix} \ddot{x}_g(t),$$

where $z_1(t) = x(t)$ and $z_2(t) = \dot{x}(t)$.

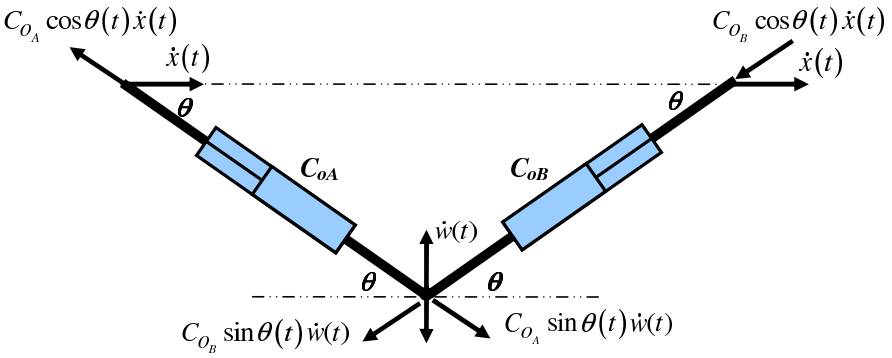

Figure 2. End velocities of the VDSA device installed in an SDOF structure.

These state-space equations can be solved by decoupling them with the complex eigenvectors of the matrix in the right hand side, provided that the displacement $w(t)$ of the bottom support of the dampers is known. The term $w(t)$ is determined by using one of the two modified algorithms Qv described in the previous section.

For practical reasons, the position $w(t)$ of the common joint of the VDSA device (which governs the damping provided to the structure), must be bounded between two limiting values $w_{\min}$ and $w_{\max}$. Thus the effective instantaneous damping in the structure can be represented by a dashpot with a variable coefficient given by

$$C(t) = \begin{cases} C_s + (C_{o_A} + C_{o_B}) \frac{a^2}{a^2 + [H - w_{\min}]^2}, & \text{for } w(t) < w_{\min}, \\ C_s + (C_{o_A} + C_{o_B}) \frac{a^2}{a^2 + [H - w(t)]^2}, & \text{for } w_{\min} < w(t) < w_{\max}, \\ C_s + (C_{o_A} + C_{o_B}) \frac{a^2}{a^2 + [H - w_{\max}]^2}, & \text{for } w(t) > w_{\max}. \end{cases} \tag{7}$$

4. Equations of motion of MDOF structures controlled with the VDSA device

The application of the VDSA device to MDOF systems is similar to the SDOF case. When the VDSA device is installed between the ith and $i+1$th building floors (and above the first level), the damping force generated by the VDSA device is related to the velocities $\dot{x}_i(t)$, $\dot{x}_{i+1}(t)$ and $\dot{w}(t)$ as shown in Figure 3.

The equation of motion for a MDOF system with the device installed between the ith and $(i+1)$th floor is

$$[M]\{\ddot{x}(t)\} + \big([C_s] + [C_1] + [C_2]\big)\{\dot{x}(t)\} + [K]\{x(t)\} = -[M]\{r\}\ddot{x}_g(t) - \{D\}\dot{w}(t). \tag{8}$$

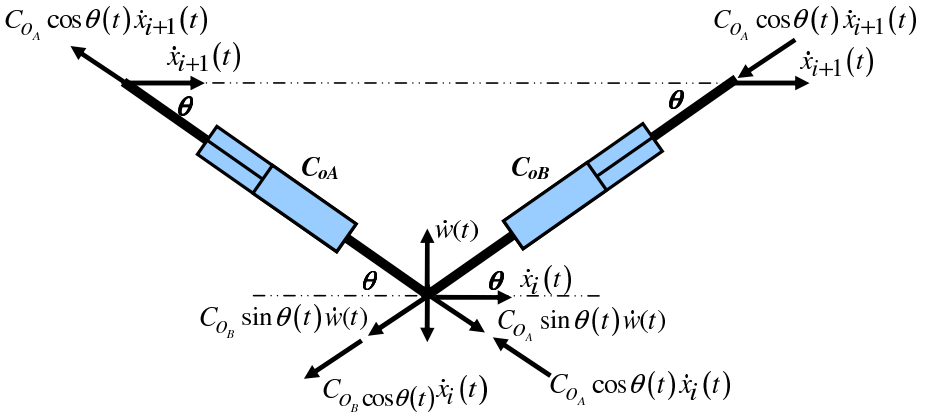

Figure 3. End velocities of the VDSA device installed between two floors of an MDOF building.

The matrices $[C_1]$ and $[C_2]$ and the vector $\{D\}$ are defined in terms of three vectors with only one or two nonzero elements. The vectors $\{e_1\}$, $\{e_2\}$ and $\{e_3\}$, with length n, are:

$$\begin{aligned}
\{e_1\}^T &= [0, 0, \ldots, 0, 1, 0, \ldots, 0] && \text{with 1 at column } i+1\\
\{e_2\}^T &= [0, 0, \ldots, 0, -1, 0, \ldots, 0] && \text{with } -1 \text{ at column } i\\
\{e_3\}^T &= [0, 0, \ldots, 0, -1, 1, \ldots, 0] && \text{with } -1 \text{ at column } i,\ 1 \text{ at column } i+1.
\end{aligned} \tag{9}$$

Using the three vectors in Equation (9), the matrices $[C_1]$ and $[C_2]$ and the vector $\{D\}$ can be written as:

$$\begin{aligned}
[C_1] &= \left(C_{o_A} + C_{o_B}\right)\cos^2\theta(t)\{e_1\}\{e_3\}^T,\\
[C_2] &= \left(C_{o_A} + C_{o_B}\right)\cos^2\theta(t)\{e_2\}\{e_1\}^T,\\
\{D\} &= \frac{1}{2}(C_{o_A} - C_{o_B})\sin 2\theta(t)\{e_1\}.
\end{aligned} \tag{10}$$

Substituting Equation (10) into Equation (8) and solving for $\{\ddot{x}(t)\}$ leads to

$$\{\ddot{x}(t)\} = -[M]^{-1}\left([C_s] + [C_1] + [C_2]\right)\{\dot{x}(t)\} - [M]^{-1}[K]\{x(t)\} - [M]^{-1}\{D\}\dot{w}(t) - \{r\}\ddot{x}_g(t). \tag{11}$$

Defining four matrices $[A_c]$, $[B_c]$, $[D_c]$, and $[E_c]$ as follows

$$\begin{aligned}
[A_c] &= -[[M]^{-1}[K]],\\
[B_c] &= -\left[[M]^{-1}([C_s] + [C_1] + [C_2])\right],\\
[D_c] &= -[[M]^{-1}\{D\}],\\
[E_c] &= [\{r\}],
\end{aligned}$$

and introducing the components of a state vector$\{z_1(t)\} = \{x(t)\}$, $\{z_2(t)\} = \{\dot{x}(t)\}$, Equation (11) can be written as:

$$\{\dot{z}_2(t)\} = [A_c]\{z_1(t)\} + [B_c]\{z_2(t)\} + [D_c]\dot{w}(t) - [E_c]\dot{x}_g(t). \tag{12}$$

To obtain the equations of motion in the state-space form, Equation (12) is supplemented with the following identity:

$$\{\dot{z}_1(t)\} = \{z_2(t)\}. \tag{13}$$

Equation (12) and Equation (13) can now be combined into the following equation of motion in the state-space:

$$\left\{\begin{array}{c}\dot{z}_1(t)\\ \dot{z}_2(t)\end{array}\right\} = \left[\begin{array}{c|c}[O_c] & [I_c]\\ \hline [A_c] & [B_c]\end{array}\right]\left\{\begin{array}{c}z_1(t)\\ z_2(t)\end{array}\right\} + \left[\begin{array}{c}[O_c]\\ \hline [D_c]\end{array}\right]\dot{w}(t) - \left[\begin{array}{c}[O_c]\\ \hline [E_c]\end{array}\right]\{\dot{x}_g(t)\}.$$

The vertical position of the lower end of the VDSA device $w(t)$ required in each instant of time, along with the damping coefficient for the coupled system, can be computed with Equation (7) using one of the two modified algorithms Qv.

5. Numerical examples

Two examples are presented in this paper to illustrate the effectiveness of the VDSA device in reducing the seismic response: an SDOF system and an MDOF structure. The response obtained by applying the

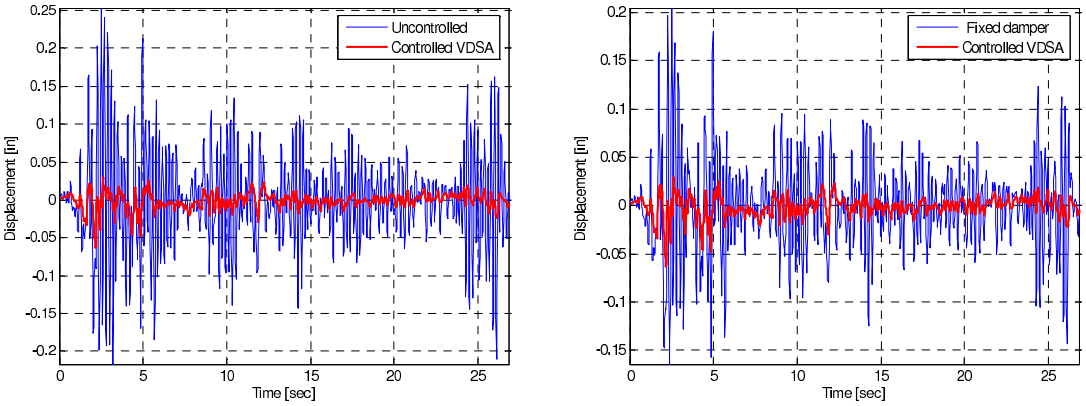

Figure 4. Left: relative displacement of the SDOF system due to the El Centro record for uncontrolled versus VDSA; right: fixed damper versus VDSA (closed-loop control).

closed-loop control modified algorithm Qv and the closed-open-loop control modified algorithm Qv are compared against the response of the uncontrolled structures. In addition, the response of the structures fitted with passive dampers is included in the comparisons. The structures are subjected to the horizontal component of three different earthquakes. First, the record of the well-known El Centro earthquake in the Imperial Valley, California on May 18, 1940, is considered. This record had a peak ground acceleration (PGA) of 0.348 g. Next, the record of the San Fernando, California earthquake of February 9, 1971, with a PGA of 1.007 g is used. Finally, the record of the Friuli, Italy earthquake of May 6, 1976, with a PGA of 0.4788 g is applied to the structures. The accelerations are sampled at equal time intervals of 0.02 sec.

Example 1. The first example is a SDOF frame with a weight of 13,630 kip and natural period of 0.20 sec. The damping coefficient of the dampers $\boldsymbol{A}$ and $\boldsymbol{B}$ of the VDSA device were 20 kip·sec/in and 10 kip·sec/in, respectively. The results obtained are compared with those of the uncontrolled structure with a damping ratio of 5%. The weighting matrix $\boldsymbol{Q}$ is selected as $[I] \times 10^2$, where $[I]$ is the identity matrix. The matrices $\boldsymbol{Qv}$ and $\boldsymbol{R}$ become scalars with values equal to 10^1 and 10^{-4}, respectively. The original damping ratio of the structure in which the VDSA system was installed was taken to be 2%. For this case of passive damping, the damping ratio was set equal to 30%, and the damping coefficient of the dampers is 40 kip·sec/in.

The response of the SDOF system to the base acceleration of the El Centro earthquake is presented first. Figure 4 shows a comparison of the relative displacement time histories for the uncontrolled structure (left), the structure with fixed dampers, and the structure controlled with the VDSA device (right). Only the first twenty-seven seconds of the response are shown. Figure 5 (left) presents the total shear force at the base of the structure as a function of time for the uncontrolled structure and the structure controlled with the VDSA device. The time variation of the position of the lower end of the VDSA device, $w(t)$, is presented in Figure 5 (right). In this case the graph shows the variation of the position of the device for the full duration of the earthquake excitation.

It can be noticed from Figure 5 (right) that the displacement $w(t)$ of the lower end of the VDSA device needs to change quite rapidly, actually in fractions of a second. This may pose a problem if a hydraulic actuator is used to push or pull the VDSA device because it may require an actuator with very

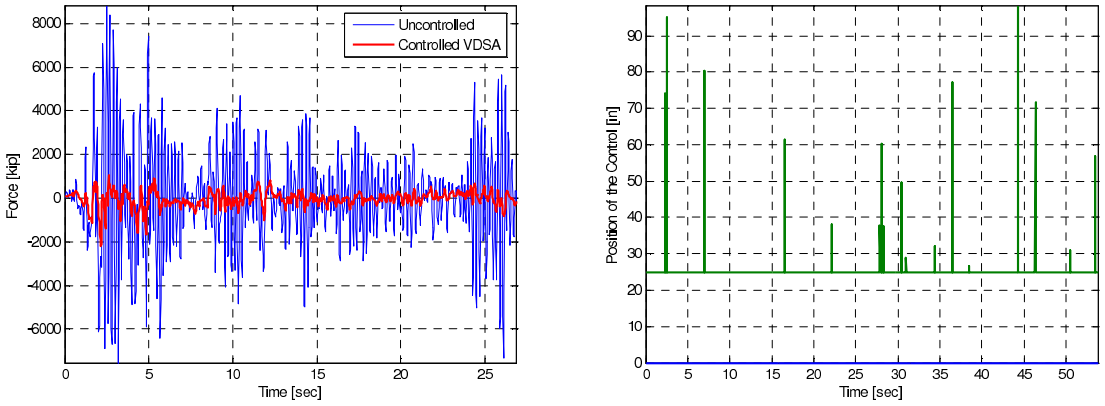

Figure 5. Left: uncontrolled versus VDSA-controlled base shear of the SDOF system. Right: variation of the position of the VDSA device for the El Centro record (closed-loop control).

high performance characteristics. In any case, for future work, and before an experimental verification of the proposed protective system is undertaken, one would ideally include a model of a nonideal actuator to study its effect on the response reduction.

The fact that the VDSA device continues to move even when the excitation diminishes (Figure 5 (right)) may be intriguing at first sight. The reason for this behavior is that both control algorithms try to minimize the response even if its magnitude is not large. In other words, during the strong motion part of the ground acceleration the semiactive control system reduces the response of the structure by about the same degree than during the final phase of the excitation. In theory, to avoid this behavior one could use in the definition of the performance index weighting matrices that vary with time. However, this will considerably increase the required computational time which may, in turn, create other problems due to the time lag between the response measurement and the actuator engagement. The effect on the

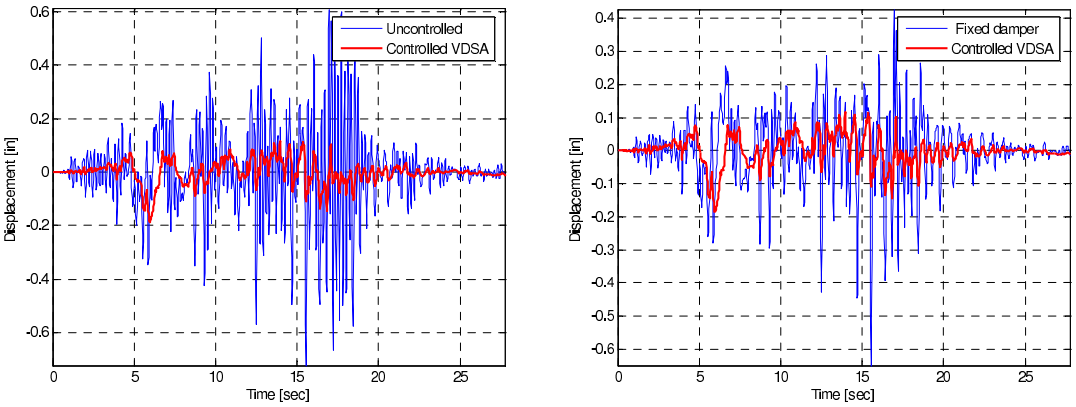

Figure 6. Relative displacement of the SDOF system for the San Fernando record for (left) uncontrolled versus VDSA, and (right) fixed damper versus VDSA (closed-loop control).

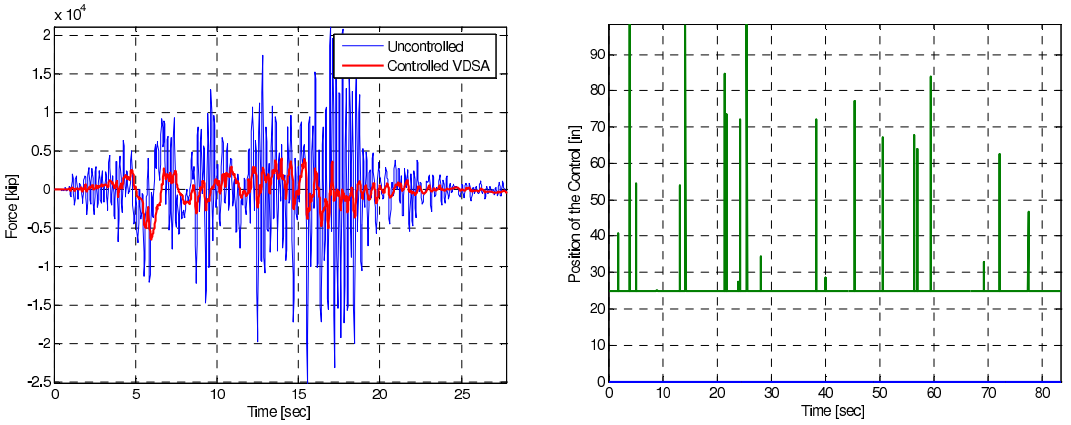

Figure 7. Left: uncontrolled versus VDSA-controlled base shear of the SDOF system. Right: variation of the position of the VDSA device for the San Fernando record (closed-loop control).

structure of the feature portrayed in Figure 5 (right) during low intensity seismic motions should be studied experimentally.

The previous response calculations were repeated with the San Fernando record. The responses compared are those obtained with the original (uncontrolled) structure, with fixed dampers and with the VDSA device. Figure 6 shows the time variation of the displacements for the three conditions whereas Figure 7 (left) displays the base shear time histories. The first forty-two seconds of the response is shown. Figure 7 (right) shows the variation of the height of the lower end of the device $w(t)$ for the San Fernando earthquake. Similar observations to those made for the El Centro earthquake can also be repeated here regarding the nature of the time variation of $w(t)$.

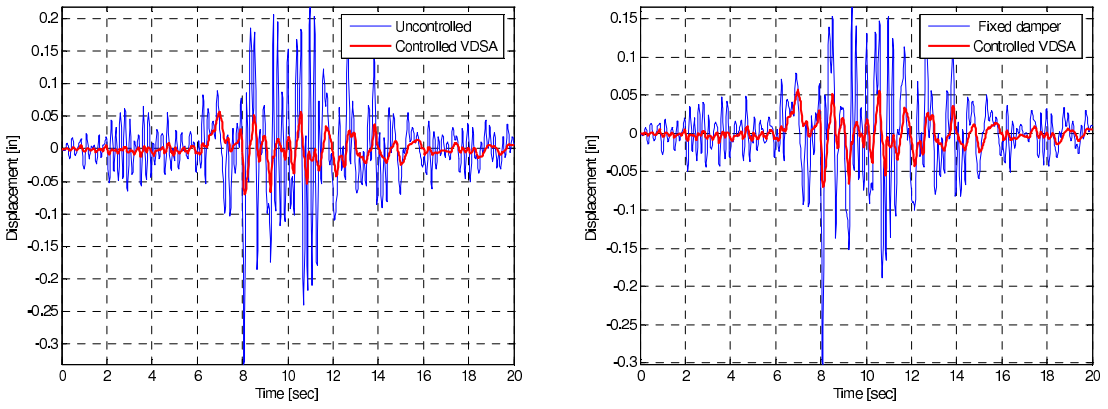

Figure 8. Relative displacement of the SDOF system for the Friuli record for (left) uncontrolled versus VDSA, and (right) fixed damper versus VDSA (closed-loop control).

Earthquake	Displacement			Total base shear		
	Uncont.	Fixed damper	VDSA	Uncont.	Damper Fixed	VDSA
	[in]	[in]	[in]	[kip]	[kip]	[kip]
El Centro	0.2536	0.2049	0.0630	8828.0	7133.1	2192.1
San Fernando	0.7219	0.7072	0.1848	25132.0	24620.0	6435.3
Friuli	0.3315	0.3019	0.0696	11540.0	10509.0	2424.3

Table 1. Maximum response of the SDOF structure without control and with a passive and semiactive system (closed-loop control).

The next set of results corresponds to the 1976 Friuli accelerogram. Again, the responses compared are the relative displacement of the mass, and the sum of the shear forces in the columns, in both uncontrolled and controlled mode with fixed dampers and with the VDSA device. The results are presented in Figure 8 and 9 (left) for the first twenty seconds of the response. Figure 9 (right), shows the variation of the position of the VDSA device.

Table 1 shows a summary of the maximum responses obtained for the SDOF structure of Section 5 when the closed-loop modified algorithm Qv was used. Table 2 is similar to Table 1 but displays the controlled response using the closed-open-loop control algorithm. Both tables demonstrate the advantages of using the VDSA device. In addition, the tables show that both the closed-loop and closed-open-loop control modified algorithms Qv provide almost the same results. The fact that both algorithms yielded similar results coincides with the results observed in the area of active structural control whenever the closed-loop and closed-open loop control formulations are used.

Example 2. A six-story building was selected to show, via a numerical simulation, the implementation of the VDSA device and to illustrate its effectiveness in reducing the seismic response of a MDOF structure. For simplicity, the structure is modeled as a shear building with one DOF per floor (the lateral

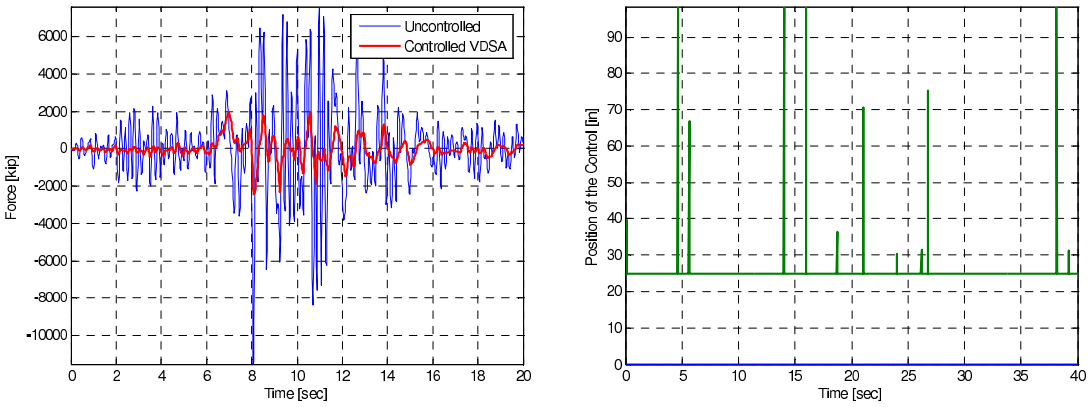

Figure 9. Left: uncontrolled versus VDSA-controlled base shear of the SDOF system. Right: variation of the position of the VDSA device for the Friuli record (closed-loop control).

Earthquake	Displacement			Total base shear		
	Uncont.	Fixed damper	VDSA	Uncont.	Fixed damper	VDSA
	[in]	[in]	[in]	[kip]	[kip]	[kip]
El Centro	0.2536	0.2049	0.0616	8828.0	7133.1	2144.5
San Fernando	0.7219	0.7072	0.1816	25132.0	24620.0	6322.2
Friuli	0.3315	0.3019	0.0678	11540.0	10509.0	2361.6

Table 2. Maximum response of the SDOF structure without control and with a passive and semiactive system (closed-open-loop control).

displacement). The total lateral stiffness coefficients of the columns are $k_i = 5,315$ kip/in and the floor weights are $W_i = 2,205$ kip. The damping ratio of the uncontrolled structure is assumed to be 5% for all the modes. For the case where the dampers are installed in a fixed position, the damping ratio provided by them is selected to be 30% for the first mode. The damping coefficients of the dampers of the VDSA device are 25 kip·sec/in and 10 kip·sec/in for the dampers A and B, respectively. The results obtained are compared with those obtained for the uncontrolled structure and also with the response calculated with fixed dampers. In the latter case three configurations, identified as I, II and III, were considered. Each corresponds to increasing number of fixed dampers: in case I, a single damper was installed at the first floor; in case II three dampers were placed on the three lower floors and in case III a damper was installed at each of the six floors. The VDSA device was assumed to be installed in the fourth floor. This position was found to be the best one by a simple trial and error process. For closed-loop and closed-open-loop control algorithms Qv the weighting matrices $\boldsymbol{Q}$ and $\boldsymbol{Qv}$ were selected as $[I] \times 10^4$ and $[I] \times 10^2$, respectively, where $[I]$ is an identity matrix. Matrix $\boldsymbol{R}$ is, in this case, a scalar with a value equal to 10^{-1}.

The first result for the MDOF structure is the response to the ground acceleration due to the 1940 El Centro earthquake. The relative displacements computed for the uncontrolled structure are compared with a similar response quantity but for the structure controlled with the VDSA device. The time trace of

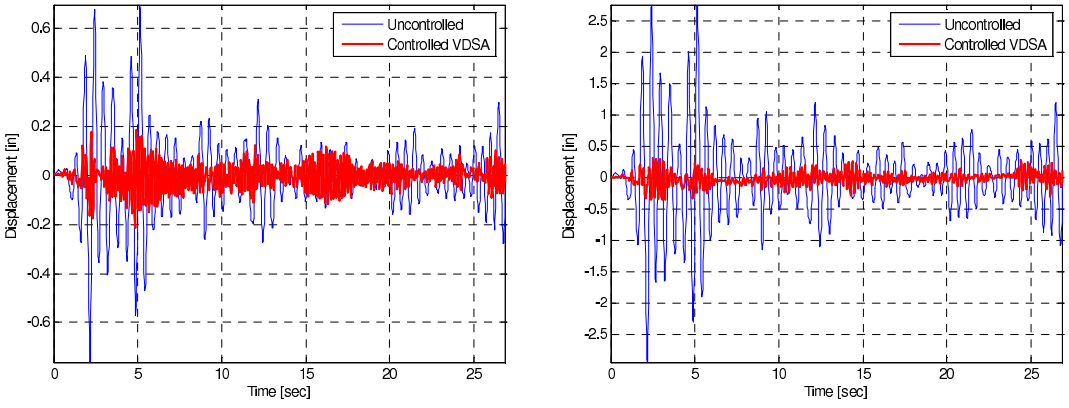

Figure 10. Relative displacements of the 6-story building for the El Centro record, (left) first floor, and (right) top floor — uncontrolled versus VDSA (closed-loop control).

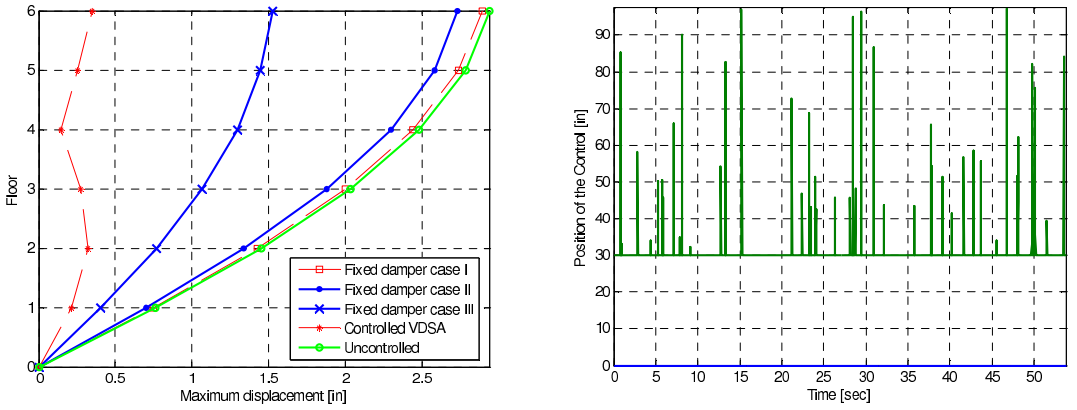

Figure 11. Left: maximum floor displacements for all cases. Right: variation of the position of the VDSA device — El Centro record (closed-loop control).

the relative displacements of the first and six floors are presented in Figure 10 (left and right, respectively). The maximum relative displacements in the six floors for all the cases considered are shown in Figure 11 (left). There are five cases considered: the original structure, the structure with a single VDSA device in the fourth floor, and the three fixed damper configurations I, II and III, previously described. Clearly, the response reduction achieved by the VDSA system is remarkable, even when compared to the case in which all floors are provided with viscous dampers at the maximum practical range. The variation of the control device position for the El Centro record is presented in Figure 11 (right).

The previous analyses were repeated for the San Fernando ground motion. Figure 12 displays the time variation of the displacement response for the first and top floor of the original structure and controlled with the VDSA device. The next set of results displayed in Figure 13 is the maximum relative displacements of the six floors for all cases studied (left) and the vertical position of the lower end of the device (right).

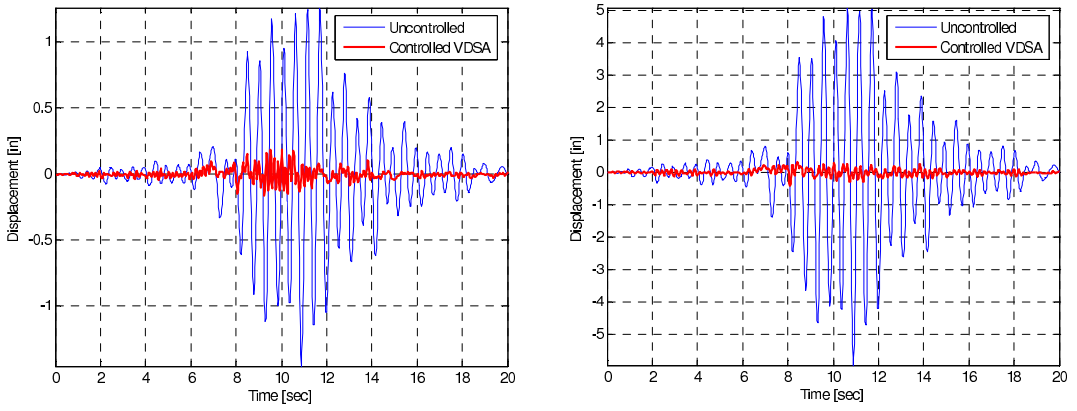

Figure 12. Relative displacements of the 6-story building for the San Fernando record, (left) first floor, and (right) top floor — uncontrolled versus VDSA (closed-loop control).

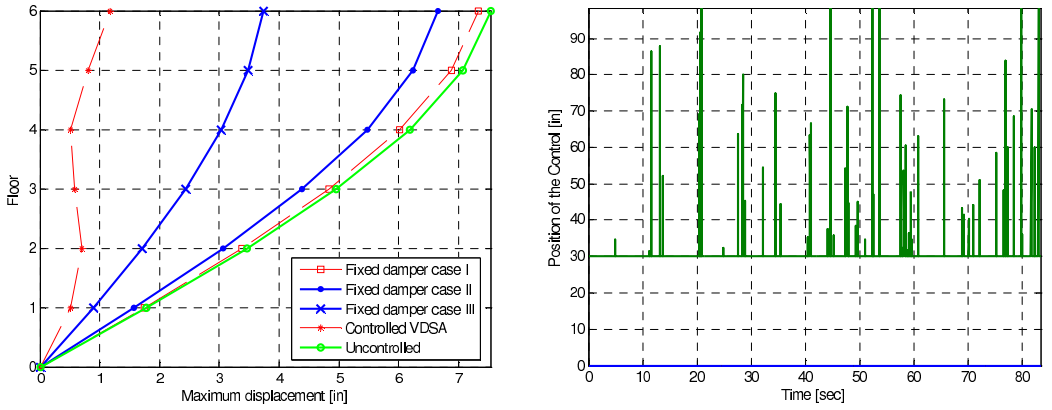

Figure 13. Left: maximum floor displacements for all cases. Right: variation of the position of the VDSA — San Fernando record (closed-loop control).

The last set of results corresponds to the response of the 6-story building subjected to the acceleration of the Friuli earthquake. Only the first twenty seconds of the response is shown. Figure 14 displays the relative displacement time histories of the structure in uncontrolled mode (left) and controlled mode (right) with the variable dampers for the first and top floor. Figure 15 shows the maximum relative displacements of the six floors for the five cases analyzed (left) and the variation of the position of the VDSA device (right).

Here also the maximum responses obtained using the closed-loop and closed-open-loop control algorithms were practically the same. Only small differences in the form that varies the position of the VDSA device were found [Cundumi 2005].

A summary of the response of the structure in three conditions: a) uncontrolled, b) fitted with fixed (passive) dampers using the configurations I, II and III, and c) controlled with the proposed semiactive device, are compared in Tables 3–5. These tables present the maximum relative displacement for all floors when the El Centro, San Fernando, and Friuli ground motions were applied at the base. It can be

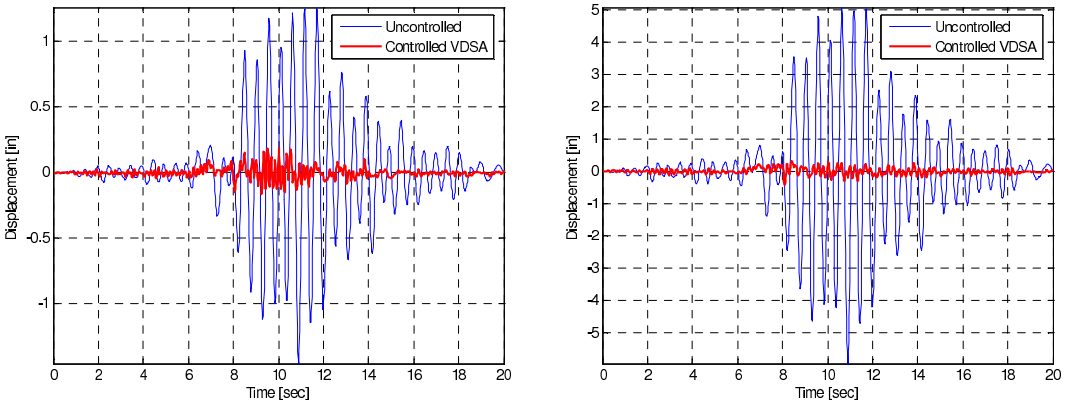

Figure 14. Relative displacements of the 6-story building for the Friuli record, (left) first floor, and (right) top floor — uncontrolled versus VDSA (closed-loop control).

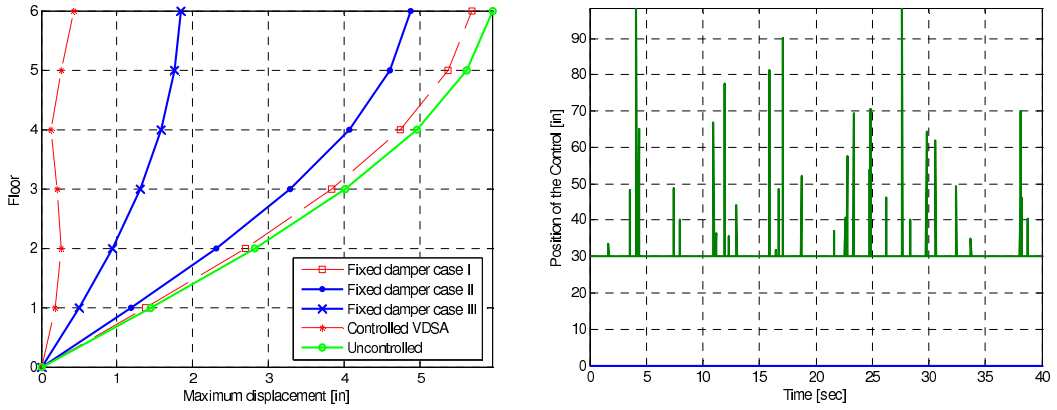

Figure 15. Left: maximum floor displacements for all cases. Right: variation of the position of the VDSA — Friuli record (closed-loop control).

noticed that the VDSA device is effective in reducing the relative displacements and shear forces. The results presented in this paper correspond to the VDSA device installed in the fourth floor where the best response reduction was obtained. However, although it is not presented here, comparable reductions were obtained with the VDSA device positioned in other floors. As expected, the best results obtained with passive control were for case III in which the dampers were installed in all six floors of the building. In this passive case the fixed dampers were assigned a damping coefficient equal to the maximum recommended practical limit. The reduction in the maximum displacements of the building with the VDSA device compared to the passive control (case III) ranges from 50–80%. When the maximum displacement reduction achieved with the proposed system is compared with the original structure, the decrease in the top floor response varies from 88–93%.

Finally, the effectiveness in the response reduction in MDOF structures with the VDSA device controlled by the modified closed-loop and closed-open-loop control algorithm Qv was observed to be the same. In other words, in terms of performance, there was no advantage in using one methodology over the other.

Floor	Displacement				
	Uncont.	Fixed damper Case I	Fixed damper Case II	Fixed damper Case III	VDSA
	[in]	[in]	[in]	[in]	[in]
6th	2.939	2.894	2.732	1.529	0.352
5th	2.786	2.742	2.586	1.448	0.252
4th	2.483	2.443	2.301	1.296	0.141
3rd	2.036	2.000	1.881	1.069	0.273
2nd	1.454	1.427	1.340	0.769	0.320
1st	0.762	0.747	0.700	0.405	0.215

Table 3. Maximum displacements of the 6-story building without control and with a passive and semiactive system for the El Centro record (closed-loop control).

Floor	Displacement				
	Uncont.	Fixed damper Case I	Fixed damper Case II	Fixed damper Case III	VDSA
	[in]	[in]	[in]	[in]	[in]
6th	7.528	7.321	6.650	3.731	1.178
5th	7.066	6.873	6.244	3.485	0.800
4th	6.185	6.018	5.467	3.035	0.519
3rd	4.957	4.823	4.380	2.432	0.585
2nd	3.463	3.371	3.057	1.715	0.701
1st	1.785	1.738	1.575	0.897	0.519

Table 4. Maximum displacements of the 6-story building without control and with a passive and semiactive system for the San Fernando record (closed-loop control).

Floor	Displacement				
	Uncont.	Fixed damper Case I	Fixed damper Case II	Fixed damper Case III	VDSA
	[in]	[in]	[in]	[in]	[in]
6th	5.951	5.689	4.877	1.850	0.428
5th	5.617	5.369	4.602	1.759	0.271
4th	4.960	4.741	4.063	1.579	0.132
3rd	4.010	3.832	3.283	1.307	0.210
2nd	2.813	2.688	2.304	0.946	0.269
1st	1.452	1.383	1.184	0.505	0.186

Table 5. Maximum displacements of the 6-story building without control and with a passive and semiactive system for the Friuli record (closed-loop control).

6. Conclusions

The results presented in Tables 1 and 2 for the SDOF structure, selected as the first example, indicate that the maximum relative displacements due to the El Centro, San Fernando, and Friuli accelerograms were reduced by 75.2%, 74.4%, and 79.0%, respectively, compared to the case when the structure had its original 5% damping ratio. The results were obtained by using the modified closed-loop control algorithm Qv. When the modified closed-open-loop control algorithm Qv was used to define the position of the VDSA device, the reductions were 75.7%, 74.8% and 79.6%, that is, practically the same. When compared to the case in which the SDOF system was fitted with fixed dampers, the peak relative displacements were reduced by 19.2%, 2.0%, and 8.9% for the El Centro, San Fernando, and Friuli earthquakes.

In another example a 6-story shear building was used to numerically examine the performance of the proposed semiactive dampers. The maximum relative displacements of all floors for the three seismic records were presented in Table 3, 4 and 5, respectively. The reductions obtained with the VDSA device in the top floor displacements were 88.0% (for El Centro), 84.4% (for San Fernando) and 92.8% (for Friuli). Both algorithms led to the same results. To compare the effectiveness of the VDSA device with viscous dampers in a fixed position, three configurations were selected for the latter case. The

best results were observed when the structure had passive dampers installed in all floors (a configuration identified as Case III). In this case the reduction in the peak displacement at the top floor was 48%, 50.4%, and 68.9% for the El Centro, San Fernando and Friuli accelerograms. The reduction in the displacements of the lower floors is not as dramatic as in the top floor. However, the proposed device was capable of achieving a notable decrease even for the lowest floor. For example, the reductions in the peak displacements of the first floor obtained with the VDSA device were 71.3%, 70.9%, and 87.2% for El Centro, San Fernando and Friuli record, respectively. These percentages should be compared with the 46.8%, 49.8%, and 65.2% reduction obtained by installing fixed dampers in all the floors.

The objective of this paper was to introduce the concept of a novel variable damping device in which the damping provided to the structure can be changed by varying the orientation of two dampers with constant coefficients. A preliminary verification of the performance of the proposed device was done via numerical simulations. However, it is recognized that there are still many issues that need to be studied analytically and even more importantly, experimentally. For instance, the actuator was assumed to be ideal, that is, no actuator dynamics were included in the simulations. The final corroboration of the concept must be done through a thorough experimental program.

7. Acknowledgment

The authors would like to thank the reviewers of the paper for their valuables comments.

References

[Cundumi 2005] O. Cundumi, *A variable damping semiactive device for control of the seismic response of buildings*, Ph.D. Dissertation, the University of Puerto Rico at Mayagüez, Department of Civil Engineering, Mayagüez, Puerto Rico, 2005.

[Cundumi and Suárez 2006a] O. Cundumi and L. E. Suárez, "A new variable damping semi-active (VDSA) device for seismic response reduction of civil structures", in *The IX pan american congress of applied mechanics (PACAM IX)*, Mérida, Mexico, January 2–6 2006a.

[Cundumi and Suárez 2006b] O. Cundumi and L. Suárez, "Seismic response reduction using semi-active control with a new variable damping device and modified algorithm $\boldsymbol{Qv}$", in *Proceedings of the eight U.S. national conference on earthquake engineering*, San Francisco, California, April 18–22 2006b.

[Gluck et al. 2000] J. Gluck, Y. Ribakov, and A. N. Dancygier, "Selective control of based-isolated structures with CS dampers", *Earthq. Spectra* **16**:3 (2000), 593–606.

[Hrovat et al. 1983] D. Hrovat, P. Barak, and M. Rabins, "Semi-active versus passive or active tuned mass dampers for structural control", *J. Eng. Mech., ASCE* **109**:3 (1983), 691–705.

[Kawashima et al. 1992] K. Kawashima, S. Unjoh, H. Iida, and N. Niwa, "Effectiveness of the variable damper for reducing seismic response of highway bridges", pp. 479–493 in *Proceedings of the 2nd U.S-Japan workshop on earthquake protective systems for bridges*, PWRI, Tsukuba Science City, Japan, 1992.

[Kobori et al. 1993] T. Kobori, M. Takahashi, T. Nasu, N. Niwa, and K. Ogasawara, "Seismic response controlled structure with active variable stiffness system", *Earthquake & Eng. Struc. Dyn.* **22**:9 (1993), 925–941.

[Kurata et al. 1999] N. Kurata, T. Kobori, M. Takahashi, N. Niwa, and H. Midorikawa, "Actual seismic response controlled building with semi-active damper system", *Earthquake. & Eng. Struc. Dyn.* **28**:11 (1999), 1427–1447.

[Kurata et al. 2000] N. Kurata, T. Kobori, M. Takahashi, T. Ishibashi, N. Niwa, J. Tagami, and H. Midorikawa, "Forced vibration test of a building with semi-active damper system", *Earthquake. & Eng. Struc. Dyn.* **29**:5 (2000), 629–645.

[Nagarajaiah and Mate 1998] S. Nagarajaiah and D. Mate, "Semi-active control of continuously variable stiffness system", pp. 397–405 in *Proceedings of the 2nd world conference on structural control*, Kyoto, Japan, 1998.

[Patten et al. 1993] W. N. Patten, R. L. Sack, W. Yen, C. Mo, and H. C. Wu, "Seismic motion control using semi-active hydraulic force actuators", pp. 727–736 in *Proceedings of the ATC-17-1 seminar on seismic isolation, passive energy dissipation, and active control*, Redwood City, California, 1993.

[Patten et al. 1996] W. N. Patten, R. L. Sack, and Q. He, "Controlled semi-active hydraulic vibration absorber for bridges", *J. Struct. Eng., ASCE* **122**:2 (1996), 187–192.

[Sack et al. 1994] R. L. Sack, C. C. Kuo, H. C. Wu, L. Liu, and W. N. Patten, "Seismic motion control via semi-active hydraulic actuators", pp. 311–320 in *Proceedings of the 5th national conference of earthquake engineering*, El Cerrito, California, 1994.

[Sadeck and Mohraz 1998] F. Sadeck and B. Mohraz, "Semiactive control algorithms for structures with variable dampers", *J. Eng. Mech.* **124**:9 (1998), 981–990.

[Soong 1990] T. T. Soong, *Active structural control: theory and practice*, John Wiley & Sons, New York, 1990.

[Symans and Constantinou 1997] M. Symans and M. C. Constantinou, "Seismic testing of a building structure with a semi-active fluid damper control system", *Earthquake. & Eng. Struc. Dyn.* **26**:7 (1997), 759–777.

[Yang et al. 1987] J. N. Yang, A. Akbarpour, and P. Ghaemmaghami, "New optimal control algorithms for structural control", *J. Eng. Mech., ASCE* **113**:9 (1987), 1369–1386.

Received 22 May 2007. Accepted 23 May 2007.

ORLANDO CUNDUMI: ocundumi@caribbean.edu
Department of Engineering, Caribbean University, Bayamon Campus, P.O. Box 493, Bayamon, PR 00960, United States

LUIS E SUÁREZ: lsuarez@uprm.edu
Civil Engineering Department, University of Puerto Rico, P.O. Box 9041, Mayaguez, PR 00681-9041, United States